Transition from spiral waves to defect-mediated turbulence induced by gradient effects in a reaction-diffusion system

Chunxia Zhang,[1] Hong Zhang,[2] Qi Ouyang,[1,*] Bambi Hu,[2,3] and Gemunu H. Gunaratne[3]
[1]*Department of Physics, Peking University, Beijing 100871, China*
[2]*Department of Physics and Centre for Nonlinear Studies, Hong Kong Baptist University, Hong Kong, China*
[3]*Department of Physics, University of Houston, Houston, Texas 77204-5005, USA*
(Received 4 March 2003; published 3 September 2003)

The transition from spiral waves to defect-mediated turbulence was studied in a spatial open reactor using Belousov-Zhabotinsky reaction. The experimental results show a new mechanism of the transition from spirals to spatiotemporal chaos, in which the gradient effects in the three-dimensional system are essential. The transition scenario consists of two stages: first, the effects of gradients in the third dimension cause a splitting of the spiral tip and a deletion of certain wave segments, generating new wave sources; second, the waves sent by the new wave sources undergo a backfire instability, and the back waves are laterally unstable. As a result, defects are automatically generated and fill all over the system. The result of numerical simulation using the FitzHugh-Nagumo model essentially agrees with the experimental observation.

DOI: 10.1103/PhysRevE.68.036202 PACS number(s): 82.40.Ck, 47.54.+r, 87.19.Hh

I. INTRODUCTION

A common feature of an excitable or oscillatory system in a spatially extended medium is that it supports spirals that rotate around a topological defect [1–5]. Under certain conditions, a spiral may become unstable and spontaneously generate many defects [6–10]. An understanding of the transitions from spiral waves to defect-mediated turbulence has been of great interest in nonlinear physics. In the past three decades, insights into the behavior of temporal chaos in low-dimensional systems have been routinely gained using concepts such as strange attractors, Lyapunov exponents, and fractal dimensions [11]. However, high-dimensional spatiotemporal chaos has proven to be quite difficult to understand [12–14]. Certain breakthroughs have been made recently in this line of research. For example, Egolf and coworkers [15] have developed an analytical method to describe spiral waves in defect-mediated chaos which have over 100 dynamical degrees of freedom. Their method could be applied to other systems of defect-mediated turbulence, as will be described in this paper.

From a practical point of view, understanding the mechanism of spiral instability could have potential impacts on cardiology. Recent studies on animal hearts showed clear evidences that the transition from a ordered spiral wave to defect-mediated turbulence could be responsible for such life-threatening situations as tachycardia and fibrillation [4,16–21]. Using an excitable reaction-diffusion model to study the mechanism of fibrillation is one of the simplest and the most efficient ways to address this problem. It may provide certain insights into the mechanism of heart fibrillation.

Although numerical and analytical studies of transitions from spirals to defect-mediated turbulence have been well documented [5,12], evidences in controlled experiments are quite few. They have been observed only in a Rayleigh-Bénard convection [22] and certain reaction-diffusion systems. Three different spiral breakup scenarios are documented in experiments in a quasi-three-dimensional reaction-diffusion system (see the Sec. II for details of the system). In the first case, spiral waves in an oscillatory system become unstable due to a long wavelength instability, and they break up at locations far away from the spiral core because of the convective nature of the instability [6,7]. In the second case, spiral waves break up near the spiral core due to Doppler instability, when a Hopf bifurcation contributes to the movement of the spiral core, causing it to meander [8]. For these two cases, simulations and analysis with two-dimensional (2D) reaction-diffusion models qualitatively agree with the experimental observations, so that the instabilities are believed to be examples of 2D reaction-diffusion turbulence, and concentration gradients in the third dimension play a minor role. For the third case, a transition to spatiotemporal chaos takes place when a periodic external forcing is added and the ratio of the spiral-rotation period to that of the forcing is close to 3/2 [9]. The mechanism of this instability is not clear at present.

Only in the second case is the system in an excitable regime, that is why it might have relevance to heart fibrillation. However, a major discrepancy exists in this type of modeling: former observations of transitions to turbulence are believed to be quasi-two-dimensional while heart tissue is a 3D object. According to certain observations and numerical simulations, the 3D effect plays a crucial role in heart fibrillation [16]. Here we report an experimental observation of a transition to defect-mediated turbulence due to 3D effects, where the gradients in the third dimension play an essential role. The transition scenario consists of two stages: first, the effects of gradients in the third dimension cause the splitting of the spiral tip and a deletion of wave segments, generating new wave sources; second, the waves sent by the new wave sources undergo a backfire instability, and the back waves are laterally unstable. As a result, defects are automatically generated and fill all over the system. We

*Author to whom correspondence should be addressed. Email address: qi@pku.edu.cn

also conducted numerical simulations to study the gradients in the 3D reaction-diffusion system. Our result shows that introducing concentration gradients in the third dimension can induce a spiral to break up, while this spiral is stable in a 2D system.

II. EXPERIMENTAL SETUP

Our experiments were conducted in a spatial open reactor, the same as described in earlier studies [6–9]. The reaction medium is a membrane, 0.4 mm in thickness and 22 mm in diameter, made of a porous glass with an average porous size of 10 nm (Vycor glass, Corning). The porous glass disk prevents any convection motion in the reaction medium so that the reaction-diffusion feature is guaranteed in the system. Contacting each surface of the membrane with a reservoir, where reactants are refreshed continuously, fulfills a homogeneous and constant boundary condition of the reaction medium. Ferroin catalyzed Belousov-Zhabotinsky (BZ) reaction is used in the experiments. The chemicals are arranged in the two reservoirs in such a way that one (I) is kept in the reduced state of BZ reaction, the other (II) is kept in the oxidized state. When reactants of both sides diffuse in the membrane and meet together, pattern forming reactions take place in a thin layer inside the membrane, where spiral waves can be sustained.

Multiple concentration gradients exist across the membrane, so that the system is a 3D system with gradients in the third dimension. These concentration gradients can induce instabilities in the system [23]. In our previous studies [6–9], boundary conditions were carefully chosen such that the patterned layer is thin (it is estimated to be less than 0.2 mm from the CSTR experimental data), so that the waves in this dimension are well entrained [24] and instabilities in this dimension could be avoided. In this work, we deliberately increase the thickness of the patterned layer so that dynamic instability in the gradient direction is considered. The control parameters of the experiment are the concentrations of sulfuric acid and malonic acid in reservoir I ($[H_2SO_4]_0^I$,$[CH_2(COOH)_2]_0^I$). The thickness of the patterned layer increases with $[H_2SO_4]_0^I$. According to the CSTR experimental data, it changes from less than 0.2 mm to 0.3 mm as the control parameter varies. As a result, a gradual transition from a quasi-2D system to a quasi-3D system can be obtained and the effects of concentration gradients in the third dimension can be studied. The other parameters are kept fixed: $[NaBrO_3]_0^{I,II}=0.3M$, $[KBr]_0^I=60$ mM, $[H_2SO_4]_0^{II}=0.2M$, $[\text{ferroin}]_0^{II}=1.0$ mM. The reaction temperature is $25\pm0.5\,^{\circ}$C, and the resident time in each reservoir is 10^3 s.

The initial condition of the experiment is arranged in such a way that only one spiral tip is located in the center of the reaction medium. This condition can be achieved by using a helium-neon laser (3 mW,$\lambda=633$ nm) to generate and guide spiral tips. In a regime of stable spiral, after suitable reactant solutions are pumped into reservoirs, a train of traveling waves automatically appears from the boundary of the reaction medium. We use a beam of laser light to break a chemical wave front, creating a couple of defects, which develop into a pair of counter-rotating spiral waves. Then we use laser light to lead one spiral tip to the edge of the reactor and eliminate it and drive the other one to the center of the reaction medium. Once a spiral is ready, we study it by changing one reactant concentration step by step while fixing all other conditions. A record is taken after the pattern relaxes into its asymptotic state and no laser is applied for a sufficient amount of time (around 1 h).

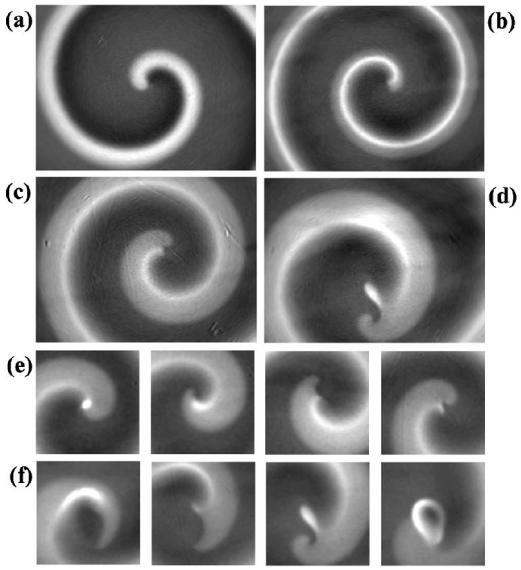

FIG. 1. Images illustrate the dimensionality of spiral changes from a quasi-2D to quasi-3D system as the control parameter increases. $[H_2SO_4]_0^I$ in (a) 0.3M, a quasi-2D spiral; (b) 0.4M, beginning of a quasi-3D spiral; (c) 0.5M, a well-developed quasi-3D spiral; (d) 0.6M, spiral tip split; (e) 0.5M, a time series shows periodic movement of tip separating and recombining, $\Delta t=2.5$ s; (f) 0.6M, a time series shows spiral tip split, $\Delta t=2.5$ s. The other control parameter is fixed: $[CH_2(COOH)_2]_0^I=0.6M$. The regions shown in (a)–(d) are 2.2×2.2 mm^2; in (e) and (f) 1.0×1.0 mm^2.

III. EXPERIMENTAL RESULT

At low $[H_2SO_4]_0^I$ (0.30M), we observed a simple rotational spiral, with a rotation period 17.5 s and wavelength of about 1.0 mm. Figure 1(a) gives a snapshot of the tip area of a spiral. The regions of high and low gray level (white and black) in the picture represent, respectively, the oxidized and reduced states of a BZ reaction. The oxidized region forms a spiral; it travels out as the spiral tip rotates around a small circle, which is 0.5 ± 0.1 mm, much large than the patterned layer. Under these experimental conditions, the spiral waves in the gradient direction can be considered as entrained [24]: although the concentration gradients tend to make the spiral different in the gradient direction, no obvious structure was observed in the experiment in this dimension. So one can consider it as a quasi-two-dimensional pattern. When the control parameter was increased to 0.4M, we observed a slight hint of a 3D structure. As shown in Fig. 1(b), the oxidized region of the spiral is not uniform. In the projection of the gradient direction, it appears that there are two traveling fronts along the spiral curve, one grayish and one bright.

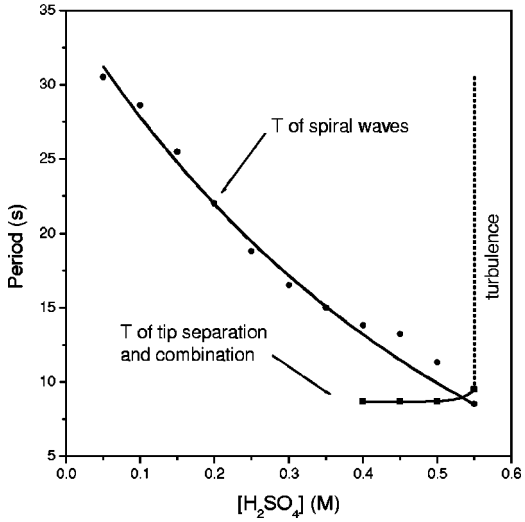

FIG. 2. The spiral period and the period of the spiral separating and recombining movement as a function of the control parameter $[H_2SO_4]_0^I$. The other control parameter is kept fixed at $[CH_2(COOH)_2]_0^I = 0.6M$.

Because the chemical compositions are different at different locations in the gradient direction, the shape of the spiral is not symmetric and its dynamic behavior is different in that direction. We observe a wider grayish spiral on one side and a narrower brighter spiral on the other side. The wavelength of the spiral is still large (0.9 mm) compared to the thickness of the reaction medium; due to spiral entrainment, the spiral waves are still stable in the gradient direction. However, in the spiral center we observe that the spiral tip tends to bifurcate. Thus the gradient effects in the third dimension must be taken into consideration. The tendency of the spiral tip to separate becomes more pronounced as the control parameter continuously increases. Figure 1(c) ($[H_2SO_4]_0^I = 0.5$ M) shows a snapshot of the situation: two separated spiral tips can be clearly seen in the region of the spiral center. A time series of pictures in Fig. 1(e) shows a periodic movement between tip splitting and recombining as the two spiral tips rotate. In this state, the rotation period of the spiral becomes 13 s, while the period of spiral tip split is 8 s; the ratio of the period of a spiral and that of tip splitting is about 3:2, but no clear signal of synchronization was observed. This splitting and recombining processes continuously intensify with the increase of $[H_2SO_4]_0^I$. When the control parameter passes across a critical value $(0.55M)$, tip splitting process wins over tip recombination process, and the two tips of the spiral separate permanently. As a result, the grayish spiral tip chips away a piece of the bright spiral tip, generating a ringlike wave with two more defects [Fig. 1(d)]. Figure 1(f) shows a time series of this process.

We have measured the period of spiral waves and that of the spiral tip splitting and recombining movement. Figure 2 summarizes the results. The period of the spiral decreases with the increase of the control parameter. The period of the spiral tip splitting and recombination stays almost constant; yet the amplitude of the movement increases. However, when the control parameter passes across the critical point

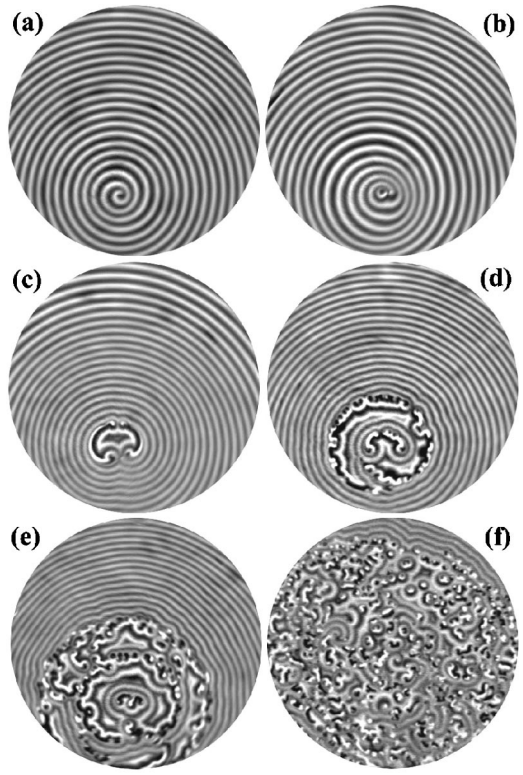

FIG. 3. Development of defect-mediated turbulence as a single spiral becomes unstable. (a) $t=0$ s; (b) $t=310$ s; (c) $t=1100$ s; (d) $t=1750$ s; (e) $t=2490$ s; (f) $t=5370$ s. The control parameters are the same as in Fig. 1(d). The region shown is 20 mm in diameter.

$(0.55M)$, the tip splitting period clearly increases, eventually becoming larger than that of the spiral wave [see Fig. 2]. At the same time, the spiral tip breaks up. The whole process looks like the following: Below the critical value of the control parameter, there are two stable spirals in the different layers of the reaction medium in the gradient direction. They travel along together due to the mutual influence of diffusive coupling. Above the critical point, this spiral entrainment breaks up because the diffusive coupling cannot compensate the difference of the two spiral waves, and they tend to separate from each other.

The spiral tip splitting process triggers a cascade of spiral dynamic changes, leading to a transition from a state of ordered spiral waves to a state of defect-mediated turbulence. Figure 3 shows the pattern evolution when the control parameter is beyond the onset. At the beginning, we have a regular spiral [Fig. 3(a)]. After the tip splitting process takes place, a ringlike wave is created [Fig. 3(b)]. The wave generated from tip splitting has different dynamical behavior, it immediately undergoes a backfire instability [25,26]. As the wave travels outward from the central region, it creates and sends a wave backward. The traveling speed of the newly created outward wave is larger than the wave speed before the onset. Its wavelength is thus smaller [compare patterns in the outer region with that near the central region in Fig. 3(c)]. The traveling speed of the newly created inward waves is smaller so that the ''hole'' in the former spiral tip region becomes larger [compare Figs. 3(b) and 3(c)]. After the

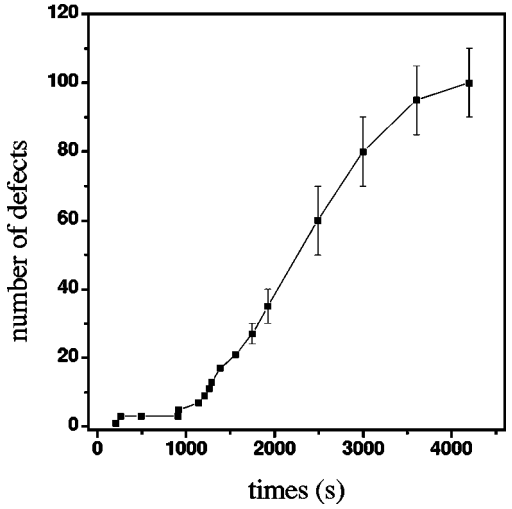

FIG. 4. Number of defects in the system measured as a function of time during the growth of the turbulent region in Fig. 3.

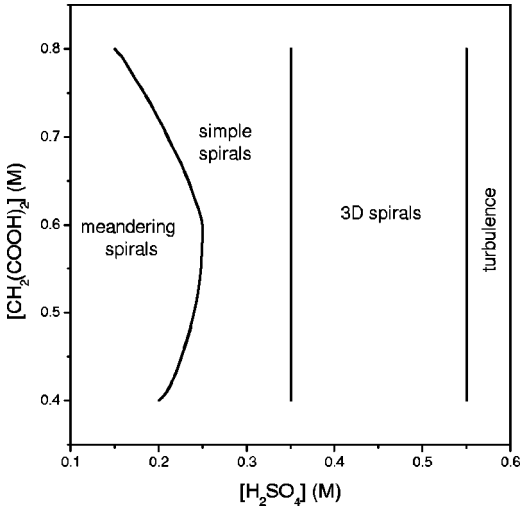

FIG. 5. The phase diagram with $[H_2SO_4]_0^I$ and $[CH_2(COOH)_2]_0^I$ as the control parameters. Regions of different patterns are indicated in the plot.

''hole'' region becomes large enough, we witness another instability of the inward wave. As the waves travel, they continuously break into pieces, generating a ring of defects [see Fig. 3(d)]. Some of the defects drift to the zone of the former spiral center, organizing new spirals. These spirals undergo the same instabilities, generating the second ring of defects [see Fig. 3(e)]. Finally, the system is full of spiral defects, we observe a state of defect-mediated turbulence, as shown in Fig. 3(f). The total transition process takes about 90 min.

During the transition, we monitored the number of defects N as a function of time in the whole reaction medium. The result is shown in Fig. 4. After an initial quick growth phase ($t<1200$ s), the growth rate of the number of defects becomes almost constant (1200 s$<t<$3500 s). Assuming that the rate of expansion of the turbulent region into the region of spiral waves is diffusion controlled, we have $l\propto\sqrt{t}$, so that $dA/dt\propto ldl/dt=$const, where A and l are, respectively, the area and the perimeter of the turbulent region. A constant growth rate of the number of defects suggests that the density of defects in the turbulent region is constant ($dN/dA=$const). When the turbulent region almost occupies the whole reaction medium ($t>3500$ s), the growth rate slows down [see Fig. 4].

A series of experiments has been conducted to study the gradient effects on spiral waves. We have traced the movement of spiral tips and distinguished the dynamical behaviors of the system according to the movement. Figure 5 gives a slice of the phase diagram using $[H_2SO_4]_0^I$ and $[CH_2(COOH)_2]_0^I$ as the control parameters. The phase diagram can be divided into several domains according the observed patterns: (a) a region of meandering spirals, where the trajectory of the spiral tip is a hypocycloid or an epicycloid [27]; (b) a region of simple spiral waves, where the trajectory of the spiral tip is a small circle and the spiral can be considered as a quasi-two-dimensional object; (c) a region of 3D spirals, where two spiral tips can be observed, so that the gradient effects in the third dimension are considered, but waves in the gradient direction overlap; (d) a turbulence region. We find in Fig. 5 that the lines of transition from a simple spiral to a 3D spiral and from a 3D spiral to spiral turbulence are independent of $[CH_2(COOH)_2]_0^I$, and the only sensible control parameter in the experiments is $[H_2SO_4]_0^I$. We also noted in the experiments that sometimes the spiral breakup was not initiated from the spiral tip region but from the region away from the spiral tip. In this case, a segment of wave spontaneously decayed, generating two more defects. This process also triggered the backfire instability, as described before. This scenario is similar to that we have observed in our simulations, which will be described in the following section.

IV. MODEL SIMULATION

We conducted numerical simulations in a quasi-three-dimensional space to see the gradient effect on the spiral stability. The FitzHugh-Nagumo reaction-diffusion model [26,28] was used because it represents a general model of excitable and oscillatory system. We first begin with the simulation in two-dimensional space. The partial differential equation (PDE) is

$$\partial u/\partial t=\nabla^2 u+u(u-a)(1-u)-v,$$

$$\partial v/\partial t=\epsilon(u-dv). \tag{1}$$

Here the variables u and v represent the concentrations of the reagents; $\nabla^2=(\partial^2/\partial x^2+\partial^2/\partial y^2)$ is the Laplacian operator; a is the excitability parameter, which was the control parameter in our simulation; and d and ϵ are other parameters, they were kept fixed in the simulation ($d=1,\epsilon=0.08$). Note that ϵ specifies the ratio between the time constants of u and v, a small value of ϵ means that the reaction system is in an excitable regime or a regime of relaxational oscillation. We investigated the dynamical behavior of this 2D system with numerical simulation. The spatiotemporal behavior of each asymptotical state as a function of the control parameter a

was recorded. When a is less than -0.127, suitable initial conditions lead to a stable state of spiral waves. If the control parameter is increased beyond -0.127, spiral waves will break up via a long wavelength instability, and the system quickly falls into a state of defect-mediated turbulence. Next, we put one more spatial dimension in the system by coupling two layers of the 2D system with diffusion. The corresponding set of PDE is

$$\partial u_1/\partial t = \nabla^2 u_1 + u_1(u_1-a_1)(1-u_1) - v_1 + c(u_2-u_1),$$

$$\partial v_1/\partial t = \epsilon(u_1 - d v_1),$$

$$\partial u_2/\partial t = \nabla^2 u_2 + u_2(u_2-a_2)(1-u_2) - v_2 + c(u_1-u_2),$$

$$\partial v_2/\partial t = \epsilon(u_2 - d v_2). \qquad (2)$$

Here u_1, v_1 and u_2, v_2 are, respectively, the variables in layer 1 and layer 2, and c is the coupling. We also induced a gradient in the newly added dimension by giving different values of a for each layer ($a_1 \neq a_2$). Thus, decoupling the two subsystems, the spiral dynamics in each subsystem is different. We will show that although the values of a_1 and a_2 are in the regime of stable spiral when the system is decoupled ($c=0$), at suitable values of the coupling strength, the coupled system can become unstable. The spirals will break up, a backfire instability will occur, and the transition to defect-mediated turbulence will take place.

In our simulations, we prepared the two subsystems with the same initial condition (same spiral waves solution) but with different control parameter values, both far from the turbulence region. Under these conditions, the asymptotical state of the system is synchronized spiral waves: the spirals in the two layers get entrained, they travel together in 2D planes. This corresponds to the quasi-2D spiral that was observed in the experiments. We then studied the behavior of the coupled systems by increasing both a_1 and a_2 but with a fixed difference, $\Delta a = a_1 - a_2 = 0.012$. When the coupling strength of the two subsystems is relatively strong ($c = 0.011$) and the control parameter a_1 is below -0.13, the state of synchronized spirals is stable. However, if the value of a_1 passes across -0.13, the system undergoes a transition to a state of turbulence. Figure 6 shows different stages of this transition. Starting from initially stable spirals [Fig. 6(a)], the breakup of spiral waves takes place in regions not far from the spiral tip [Fig. 6(b)] and backfire waves are observed near that region. As the wave travels outward near that region, it continuously creates and sends a wave backward [Figs. 6(c),6(d)]. The traveling speed of the newly created outward wave is larger than the wave speed before the onset, and the wavelength becomes smaller. The same phenomena were observed in the experiments. Meanwhile, the waves sent by the spiral tip continuously break up [Figs. 6(d),6(e)] and eventually the system is full of spiral defects [Fig. 6(f)].

Figure 7 gives a section of the phase diagram of this quasi-3D system in the parameter space of c and a_1, with $\Delta a = 0.012$. The solid line separates the stable spiral region and the turbulence region in the quasi-three-dimensional system (2), while the dashed line separates the stable spiral region and the turbulence region of the two-dimensional system (1). We observe that for a relative strong coupling strength, the two coupled spirals will always be stable even if the parameter of one subsystem is in the turbulence region. The most interesting region is the one between the dashed line and the solid curve. In this region, although both the parameters a_1 and a_2 of the two decoupled subsystems are in the region of stable spirals, the coupled spirals are not stable;

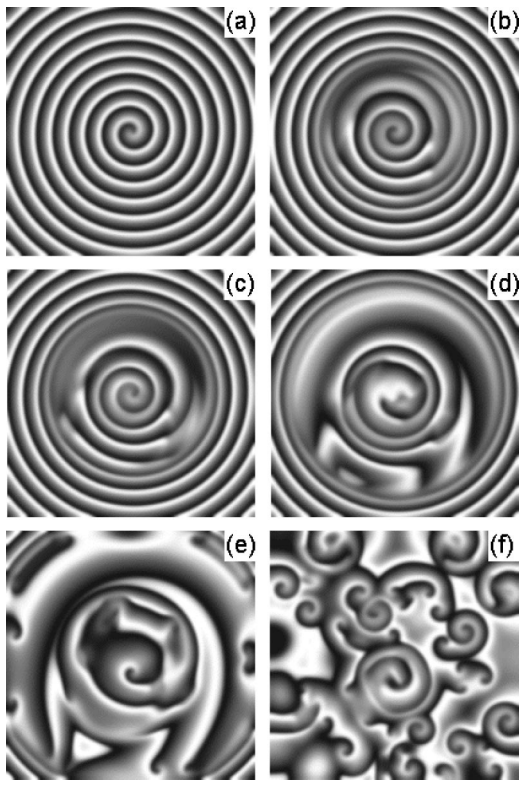

FIG. 6. The sequence of pictures shows different stages of the transition from spiral waves to defect-mediated turbulence in the simulation. The spatial patterns are a gray scale plot of (u_1+u_2). (a) $t=0$ t.u.; (b) $t=920$ t.u.; (c) $t=1010$ t.u.; (d) $t=1265$ t.u.; (e) $t=1600$ t.u.; (f) $t=3500$ t.u. The coupling strength $c=0.015$. The system size is 512×512, grid 512×512 points, and $\Delta t=0.1$. A no-flux boundary condition is imposed.

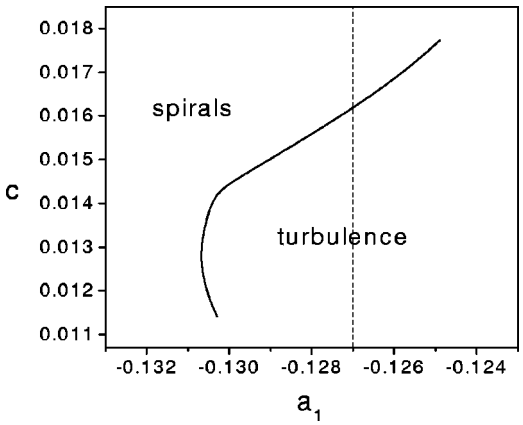

FIG. 7. A section of the phase diagram of the quasi-3D system (2) in the parameter space of c and a_1, with $\Delta a = 0.012$.

they break up and the system becomes turbulent. This is just the gradient-induced instability of quasi-3D spirals. This simulation result is consistent with our experimental observations.

V. DISCUSSION

We speculate that in the experiments the second instability which generates a ring of defects is a lateral instability [29]. Previous theoretical studies of reaction-diffusion equations show that for a first-order approximation, the speed of traveling waves in the normal direction (c_N) can be expressed in the form of the eikonal equation: $c_N = c_\infty - D\kappa$, where c_∞ is the traveling speed of a plane wave, κ is the curvature of the wave front, and D is a constant. A positive constant D guarantees that a traveling wave is stable. Suppose a perturbation is added to the system so that the curvature of the wave front becomes nonuniform, a positive value of D in the eikonal equation makes the waves in a region with a larger curvature move slower so that the curvature in that region decreases. This mechanism guarantees that the curvature of spiral wave and its speed are uniform. On the contrary, when D is negative, the waves in a region with a larger (smaller) curvature will travel faster (slower). As a consequence, the curvature in that region will be further increased (decreased). Due to slowing down of the wave speed in regions with a smaller curvature, the local wavelength in these regions becomes smaller. When the local wavelength is decreased below a critical value, which is determined by the dispersion relation [30], the traveling waves in these regions will break up and pairs of defects will be generated. Figure 8 shows an example of the lateral instability of an inward wave observed in the experiment. When the ''hole'' region in the system is small, the front of the back wave is uniform, as shown in Fig. 8(a). As the ''hole'' region becomes larger, the curvature of the back wave becomes smaller. The front at one local place [arrow pointed in Fig. 8(b)] is flatter than the other regions. Due to a negative value of D, the speed of the inward wave in the flat region is faster than its adjacent regions [Fig. 8(c)], making the local wavelength in the adjacent regions smaller. As a result, the wave breaks up in these regions and a pair of defects is created, as shown in Fig. 8(d).

In conclusion, we have observed and studied a transition from ordered spirals to defect-mediated turbulence in a controlled experiment and in numerical simulations. In the experiments, there is a clear evidence that the transition is initiated by the gradient effects of the system. These gradient effects cause the spiral tip to split or a segment of wave to decay. This triggers a cascade of spiral dynamical changes inducing backfire instability and lateral instability. As a result, the system evolves into a state of spatiotemporal chaos. In the simulation, we did not observe the spiral tip splitting; however, the following spiral breakup processes agree essentially with the experimental observation. At present, our description of the transition is still qualitative and the picture of the spiral instability is still fragmented. For example, it is not clear why the spiral tip splitting changes the dynamics of the system, such as the dispersion relation (wavelength becomes smaller) and spiral stability. We believe that a large scale 3D simulation followed by a proper theoretical analysis will finally solve these problems.

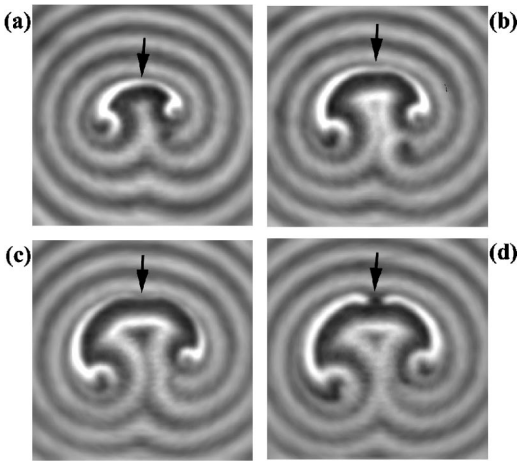

FIG. 8. Time series shows the lateral instability. The arrow points to the location where a backward wave breaks. (a) $t=0$ s; (b) $t=25$ s; (c) $t=41$ s; (d) $t=51$ s. The control parameters are the same as in Fig. 2. The region shown is 5.8×5.8 mm^2.

ACKNOWLEDGMENTS

We would like to thank H. Y. Guo for assistance in the laboratory and H. L. Swinney for providing us the porous glass disks. This work was supported in part by grants from the Chinese Natural Science Foundation (C.Z. and Q.O.), the Hong Kong Research Grants Council and the Hong Kong Baptist University Faculty Research Grant (H.Z. and B.H), and the National Science Foundation and the office of Naval Research (G.G.).

[1] A.T. Winfree, J. Theor. Biol. **138**, 353 (1989).
[2] J.P. Kneener, J. Appl. Math. **46**, 1039 (1986).
[3] M. Gerhardt, H. Schuster, and J.J. Tyson, Science **247**, 1563 (1990).
[4] J.M. Davidenko, A.V. Pertsov, R. Salomonsz, W. Baxter, and J. Jalife, Nature (London) **355**, 349 (1992).
[5] *Chemical Waves and Patterns*, edited by R. Kapral and K. Showalter (Kluwer Academic, Dordrecht, 1995), Pt. I.
[6] Q. Ouyang and J.M. Flesselles, Nature (London) **379**, 143 (1996).
[7] L.Q. Zhou and Q. Ouyang, Phys. Rev. Lett. **85**, 1650 (2000).
[8] Q. Ouyang, H.L. Swinney, and G. Li, Phys. Rev. Lett. **84**, 1047 (2000).
[9] A. Belmonte, J.M. Flesselles, and Q. Ouyang, Europhys. Lett. **35**, 665 (1996).
[10] J.S. Park and K.J. Lee, Phys. Rev. Lett. **83**, 5393 (1999).
[11] J.-P. Eckmann and D. Ruelle, Rev. Mod. Phys. **57**, 617 (1985).
[12] M.C. Cross and P.C. Hohenberg, Rev. Mod. Phys. **65**, 851 (1993).
[13] M.C. Cross and P.C. Hohenberg, Science **263**, 1569 (1994).

[14] J.P. Collub, Proc. Natl. Acad. Sci. U.S.A. **92**, 6705 (1995).
[15] D.A. Egolf, H.V. Melnikov, W. Pesch, and R.E. Ecke, Nature (London) **404**, 733 (2000).
[16] A.T. Winfree, Science **266**, 1003 (1994).
[17] R.A. Gray *et al.*, Science **270**, 1222 (1995).
[18] L. Glass, Phys. Today **49**, 40 (1996).
[19] A.V. Holden, Nature (London) **392**, 20 (1998).
[20] R.A. Gray, A.M. Pertsov, and J. Jalife, Nature (London) **392**, 75 (1998).
[21] F.X. Witkowski *et al.*, Nature (London) **392**, 7882 (1998).
[22] S.W. Morris, E. Bodenschatz, D.S. Cannell, and G. Ahlers, Phys. Rev. Lett. **71**, 2026 (1994).
[23] P. Blanchedeau, J. Boissonade, and P. De Kepper, Physica D **147**, 283 (2000).
[24] D. Winston, M. Arora, J. Maselko, V. Gáspár, and K. Showalter, Nature (London) **351**, 132 (1991).
[25] M. Bär, M. Hildebrand, M. Eiswirth, M. Falcke, H. Engel, and M. Neufeld, Chaos **4**, 499 (1994).
[26] A. Rabinovitch, M. Gutman, and I. Aviram, Phys. Rev. Lett. **87**, 084101 (2001).
[27] G. Li, Q. Ouyang, V. Petrov, and H.L. Swinney, Phys. Rev. Lett. **77**, 2105 (1996).
[28] R. FitzHugh, Biophys. J. **1**, 445 (1961).
[29] A. Hagberg and E. Meron, Phys. Rev. Lett. **72**, 2494 (1994).
[30] J.J. Tyson and J.P. Keener, Physica D **32**, 327 (1988).